Chapter - 2

Experimental Techniques

Chapter-2: Experimental Techniques

1. Introduction:

This chapter discusses the instrumentation descriptions and operating procedures of various characterizations techniques used in the present study. It is important to carry out the different characterizations to find the correct consistency and properties of the grown crystals. Characterization is the most important aspect of crystal growth because by knowing crystal's properties, one can know the usage and application of crystals in a particular field. In order to characterize the grown crystals, different methods have been used. These characterization techniques include Powder X-ray Diffraction (Powder XRD), Fourier Transform Infrared spectroscopy (FT-IR), Photoluminescence (PL), and Analysis of Dielectric properties, and Second Harmonic Generation (SHG).

2. Crystal growth:

Generally, crystal growth happens to employ the following process in the sequence:

1. In the crystallizing material, the diffusion takes place through the ambient atmosphere (or solution) to the surface of the crystal.
2. Thus, the diffusion of these modules takes place over the crystal's surface to unique sites on the surface.
3. There is an incorporation of modules at sites into a crystal.
4. There is a diffusion of crystallization phase that takes place away from the surface of the crystal.

Any of these four steps can restrict the rate of crystal growth. Nucleation is defined as the initial creation of the centres from which crystal growth progresses. A large volume of literature is available that deals with the existing hypotheses of crystal growth. Buckley [1,2] has extensively covered the mechanism of crystal growth. The crystal faces can have different surface chemistry during crystal growth and can expand through various interface kinetic mechanisms, depending on additional factors such as solvent, dopants, supersaturation, additives, etc.

In 1951, Burton, Cabera and Frank (BCF) [3] set the stage for understanding crystal growth interface structure. It made it possible to describe three mechanistic systems of crystal growth that describe the relationship between the rate of surface growth (G_R) and supersaturation (σ) thus.

a. The BCF mechanisms involve screw dislocations at low supersaturation to provide crystal surface attachment sites to allow growth at the crystal-liquid interface. The growth rate law becomes $G_R \propto \sigma^2$.

b. Surface integration will occur by two-dimensional surface nucleation through a birth and spread (BS) mechanism at moderate supersaturation. At such stage, the growth rate law becomes $G_R \propto \sigma^{5/8}$.

c. We have a rough interface growth (RIG) model at high supersaturations. Interface roughening [4] happens, and growth can continue at the interface without the need to form any well-defined surface layers. At this stage, the growth rate law becomes $G_R \propto \sigma$.

Bravaic (1866) and Friedal (1907) first suggested the basic rules for the selection of likely growth types, and Donnay and Harkar (1937) later improved them [5]. Suppose BFDH was the name given to this approach [6] which proposed the significance of crystallographic form {h k l} after allowing for space group asymmetry. In that case, it is directly dependent on the corresponding inter-planar spacings d_{hkl}. Hartman and Perdok [7] were the first to attempt to measure crystal morphology in 1955. Using their PBC (Periodic Bond Chain) theory, they measured it in terms of the interaction energy between the crystallizing units. Burton et al. [2] determined that to achieve the layer growth of an ideal crystal, a high supersaturation of at least 25-30% is required to achieve a measurable growth rate.

3. Different methods of crystal growth:

The growth of single crystals can be broadly classified into the following groups:

1. Solution Growth

a. Growth of crystals from solution

- Crystal growth from evaporation/slow cooling
- Flux growth
- Hydrothermal growth
- Liquid phase epitaxial growth

2. Melt growth

b. Growth of crystals from the melt

- Czochralski crystal pulling method
- Bridgman-Stockbargar technique
- Zone-melting and Zone-refining technique

3. Vapour growth

c. Growth of crystals from vapour

- Sublimation condensation technique
- Chemical vapour deposition (CVD)
- Metal-Organo CVD (MOCVD)
- Molecular beam epitaxy (MBE)

A slow solvent evaporation technique was used in the present investigations for growing crystals. In Chapter-1, we have briefly mentioned the crystal growth and the solution growth techniques used to grow the crystals. This work has been presented in the following sections.

4. Different experimental techniques:

- This part briefly discusses the working theory and instrumentation of various techniques used for sample characterization. The chemical composition, structure, defects, and optical properties of a crystal are determined using different characterization techniques.
- Characterization of NLO crystals can generally be divided into five types:
    1. Structural analysis of crystals
    2. Optical properties of crystals
    3. Thermal properties of crystals
    4. Non-linear properties of crystals
    5. Electrical properties of crystals
- The following experiments/characterizations were conducted on the selected single crystals for detailed investigation:
    - The unit cell parameters were obtained, and the grown crystals' composition was confirmed through powder X-ray diffraction analysis.
    - The existence of different functional groups in the crystal was confirmed using FT-IR analysis.
    - The optical transmittance and absorption of the grown crystals are measured using UV-Visible spectrum analysis, as well as the transparency region.
    - The powder second harmonic generation (SHG) experiment was used to determine the grown crystals' relative second harmonic generation efficiency.

- The thermal stability of the grown crystals was studied using Thermo-Gravimetric Analysis (TGA).
- The dielectric behaviour of the grown crystals was studied using Dielectric analysis.

5. Powder X-ray Diffraction Analysis:

Following Wilhelm Rontgen's discovery of X-rays in 1895 and the father and son pair in 1913, i.e., W. H. Bragg and W. L. Bragg provided the governing type X-ray diffraction rule known as Bragg's law. Due to which the field of crystal structure determination emerged swiftly. They showed that the diffracted beam from a crystal behaves as if the radiation is distributed by periodically aligned subatomic particles on planes acting as reflective surfaces. $2d_{hkl}$ Sin θ_{hkl} = nl, where nl is the path difference between waves scattered by adjacent lattice planes with equivalent indices; d_{hkl} is the spacing between two consecutive lattice planes, and e is the incident angle of the X-ray beam. Many different tiny crystals are present simultaneously when the sample is a powdered crystalline specimen. In certain crystallites, the rule of Bragg will be fulfilled so that the full diffraction pattern will be observed for every orientation of the crystalline powder for the X-ray beam.

The powder reflections sit on a semi-vertical angle θ_{hkl} cone for any given mixture of indices hkl. If a, b, c, α, β, and γ are details about the unit cell, then the values of $\text{Sin}^2\,\theta_{hkl}$ for different crystal systems are given by Steeple and Lipson [8].

1) Cubic System

$$\text{Sin}^2\,\theta_{hkl} = \frac{\lambda^2}{4a^2}(h^2 + k^2 + l^2)$$

2) Tetragonal System

$$\text{Sin}^2\,\theta_{hkl} = \frac{\lambda^2}{4a^2}(h^2 + k^2) + \frac{\lambda^2}{4c^2}l^2$$

3) Hexagonal System

$$\text{Sin}^2\,\theta_{hkl} = \frac{\lambda^2}{3a^2}(h^2 + hk + k^2) + \frac{\lambda^2}{4c^2}l^2$$

4) Orthorhombic System

$$\text{Sin}^2\,\theta_{hkl} = \frac{\lambda^2}{4a^2}h^2 + \frac{\lambda^2}{4b^2}k^2 + \frac{\lambda^2}{4a^2}l^2$$

5) Monoclinic system

$$\text{Sin}^2\,\theta_{hkl} = \frac{\lambda^2}{4}\frac{\left(\frac{h^2}{a^2}+\frac{l^2}{c^2}+\frac{2hl}{ac}\cos\beta+\frac{k^2}{b^2}\right)}{Sin^2\beta}$$

6) Triclinic system

$$\text{Sin}^2\,\theta_{hkl} = = \frac{\lambda^2}{4}\left[\frac{\left(\frac{h^2sin^2}{a^2}+\frac{l^2sin^2}{c^2}+\frac{k^2sin^2}{b^2}\right)}{1-cos^{\,2}\alpha-cos^2\beta-cos^2\gamma+2\,cos\,\alpha\,cos\,\beta\,cos\gamma}\right]+$$

$$\left[\frac{\frac{2hk\,(cos\,\alpha\,cos\beta-cos\gamma)}{ab}+\frac{2kl\,(cos\beta\,cos\gamma-cos\,\alpha)}{bc}+\frac{2lh\,(cos\,\alpha\,cos\gamma-cos\beta)}{ca}}{1-cos^{\,2}\alpha-cos^2\beta-cos^2\gamma+2\,cos\,\alpha\,cos\,\beta\,cos\gamma}\right]$$

where α, β, γ are the angles between b & c, c & a and a & b, respectively.

X-ray powder diffraction is an effective analytical technique commonly used for applications ranging from basic research to routine quality control in many fields of science and many industries. It is used to identify unknown materials in aspects of its crystalline structure, identify new compounds and crystalline structures, and look for nonconformities from the perfect structure that can indicate strain, impurities, crystal size, and other structural defects if present. This technique is based on the principle of constructive and destructive interference emitted by X-rays. These X-rays are emitted from a sample illuminated by a filtered and concentrated X-ray beam.

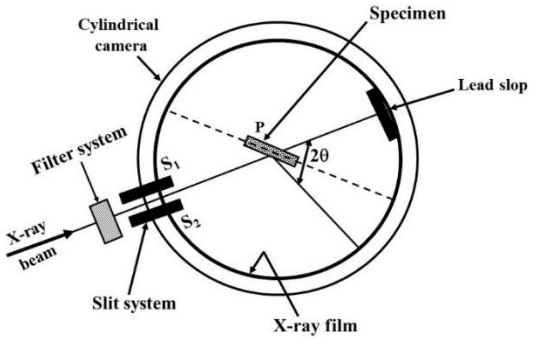

Figure 1(a). Experimental arrangement of a typical Powder XRD set-up

The experimental arrangement of the powder X-ray diffraction method is shown in figure 1(a). The key role of such a system may be ascribed as follows: A is an X-ray source that can be made monochromatic by a filter. The X-ray beam passes through the slits S_1 and S_2 and falls on the powdered specimen P. The primary function of the slits is to narrow the X-ray beam. After falling on the powder, the X-rays pass out of the camera through a cut in the film to minimize the fogging caused by the direct beam scattering. The intensity of the reflected X-rays is recorded as the powder sample and detector is rotated. When the X-rays are incident on

the sample, it satisfies Bragg's equation and constructive interference, and a peak in intensity occurs. This X-ray signal is recorded and processed by a detector, and the signal is converted to a count rate, which is then transferred to a system such as a printer or a computer monitor. In addition, the mathematical study of the relative orientation of individual crystals from an aggregate can be done using the powder X-ray diffraction technique [9]. BRUKER AXS 08 Advance model X-ray diffractometer with CuKα_1 (λ = 1.54056 Å) radiation in the 2θ range of 10° to 80° at IUC-UGC-CSIR, Indore, was used to record the powder pattern with a scanning speed of 1°/minute for the sample, and all the tests were conducted at room temperature with air as ambient.

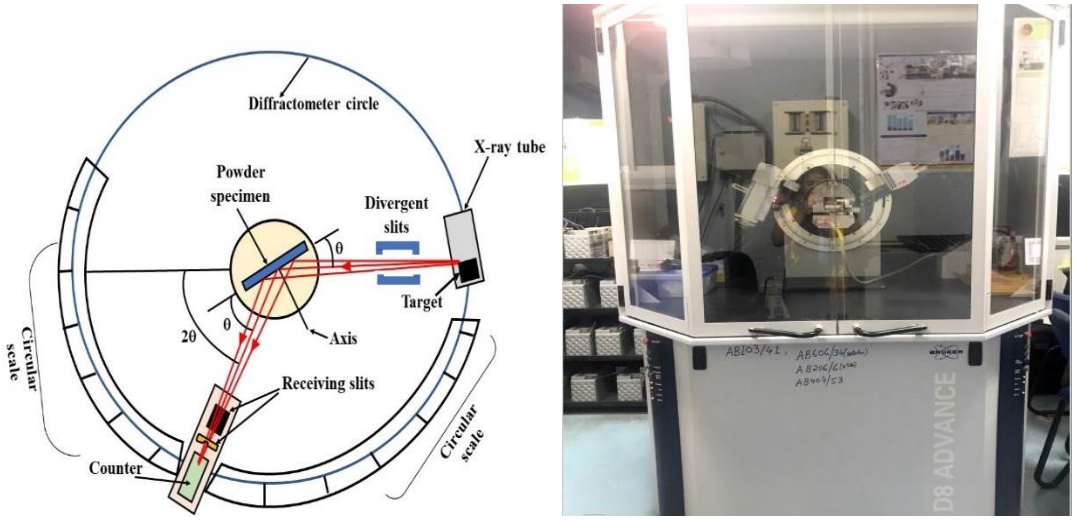

Figure 1(b). Schematic diagram of Powder X-ray Diffractometer and BRUKER AXS 08 Advance model X-ray diffractometer

6. Fourier Transform Infrared (FT-IR) Spectroscopy:

The most prominent method used to detect the vibrations of atoms in molecules and crystals is FTIR spectroscopy. The multiplicity of vibrations evolving simultaneously creates an absorption spectrum that features a molecule's functional groups and overall atom structure. Comparing the obtained spectrum with the characteristic functional group frequency, functional groups in a sample may be assigned. This involves a separate feature absorption band that belongs to the functional group describing complex substance chemical bonds. The spectra are mainly derived from molecules that have vibrational stretching and bending modes.

In this method, the molecules will undergo vibrational transitions when an infrared radiation incident on the molecules of sample material, resulting in the shift in the dipole moment of molecules. Eventually, at a particular resonance frequency, the resulting resonance absorption band occurs. The infrared region of the electromagnetic spectrum includes the red end of the visible spectrum to the microwave region. The molecular vibrations like rotating, stretching, bending, twisting, etc., are prone towards infrared (IR) radiations. The proportion of incident radiation is absorbed in a specific wavelength when the IR radiation falls on the molecule.

Due to such absorption, various vibrational transitions of molecules occur, which results in a highly complex absorption spectrum. The Fourier Transform Infrared Spectroscopy (FT-IR) technique is helpful for the Mid IR (4000-400 cm^{-1}) region. The amplitude of the vibrational band can be expressed either as transmittance (T%) or absorbance (A%) as a function of wavenumber in (cm^{-1}). Figure 3 shows that the FT-IR spectrometer is based on Michelson Interferometer, and such interferometer is fitted inside the FT-IR instrument.

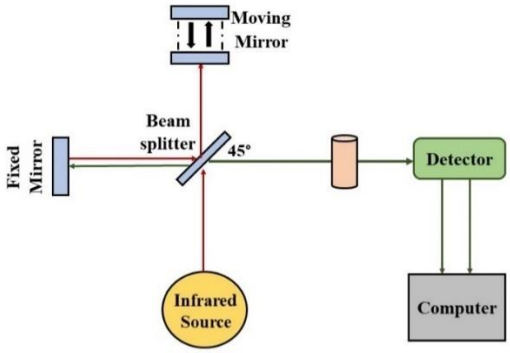

Figure 2(a). FTIR Spectrometer photograph

6.1 Working of FT-IR spectrometer:

The schematic diagram of the FT-IR spectrometer is shown in above figure 3(a). **(i)** Drive mechanism, **(ii)** Beam splitter, and **(iii)** Sources and transducers are the three main components of FT-IR spectrometer. IR radiation comes from the IR source, and the mirror collimates the beam. Then the resulting beam is separated by the beam splitter. Half of the beam is passed to the beam splitter's fixed mirror, and half is reflected to the moving mirror. The mirrors are adjusted in such a way that they are at a right angle to each other. The two reflected beams undergo interference, either constructively or destructively, depending on their path difference. The intensity of emerging radiation is modulated sinusoidally as the moving

mirror shifts with constant velocity. Now that the modulated signal is going through the sample, the detector can detect the sample's signal. Using Fourier Transform, the interferogram, i.e., the resulting signal at the detector, will be reconstructed. The computer software attached to the instrument will perform a mathematical process on the signal and plot transmittance or absorption versus wavenumbers spectrum.

In determining the forces binding the atoms of the molecule and evaluating many molecular constants, the vibrational frequencies are important. The restoring force per unit displacement, stretching or bending is defined as 'Force Constant'. It is a measure of the strength of the chemical bonding between the atoms. Certain bonding properties such as interatomic interactions and delocalization can be visualized with the help of force constant. It also helps to provide information on the valance state of the atoms in the molecule [10]. The FTIR spectrum of crystals was reported in this thesis using BRUKER Alpha-I at Parul Institute of Pharmacy, Parul University. The crystals were crushed and blended with KBr (Potassium Bromide) into a very fine powder, and KBr pellet technique was used. The FT-IR spectrometer has an optical resolution of 2 cm^{-1} in the range of 4000 cm^{-1} to 400 cm^{-1}.

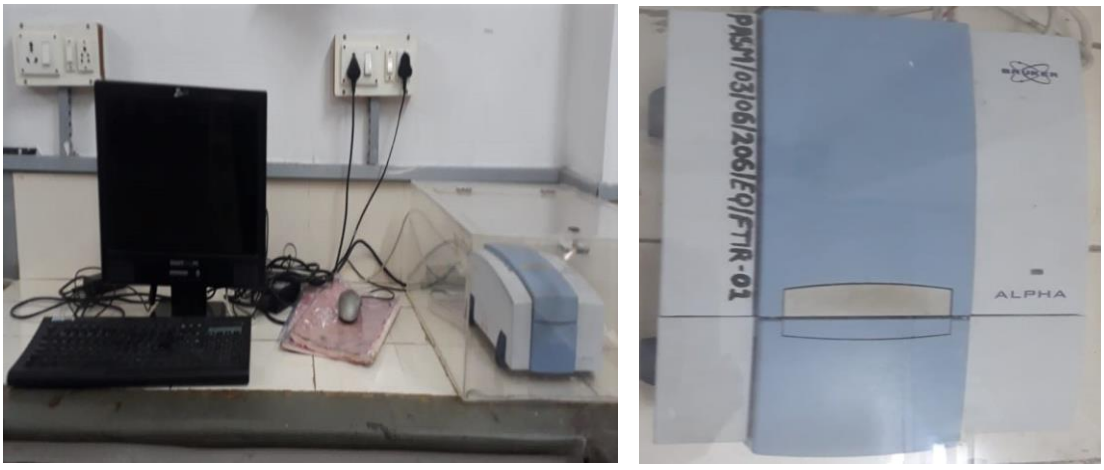

Figure 3(b). BRUKER Alpha-I

7. Ultraviolet-Visible (UV-Vis) Spectroscopy:

Electromagnetic emission in the UV-visible region is used in ultraviolet-visible (UV-Vis) spectroscopy (UV-Visible region 200-800 nm). Electronic transitions occur in this portion of the electromagnetic spectrum. Since the promotion of electrons from the ground state to the excited state of conjugated systems causes absorption in this region, UV spectroscopy is primarily used to detect such systems. Whenever UV-Visible radiation is transmitted through

a sample, absorption of energy occurs, which causes an electron to be promoted from the ground electronic state to the excited electronic state.

Many photon molecule collisions occur during the absorption process; however, only certain collisions can result in energy absorption when the photon's energy matches the energy difference between the ground state and the excited electronic state of the molecule. Thus, the amount of energy absorbed is calculated. π-Bonding orbitals, σ-bonding orbitals, and non-bonding orbital's (n-lone pair electrons) are the three groups of orbitals in which valence electrons can be found. The energy of σ-bonding orbitals is lower than that of π-bonding orbitals, which is lower than that of non-bonding orbitals. The orbitals with the highest energy are the unoccupied or anti-bonding orbitals (π* and σ*).

UV-Vis spectroscopy measures the attenuation of a light beam as it travels through a sample or after reflection from a sample surface, and this spectrum plays a critical role in determining the NLO material's ability. Once molecules of the sample are subjected to light with energy that meets a potential electronic transition within the molecule, most of the light energy is absorbed when the electron is promoted to a higher energy orbital. UV-Vis spectrophotometer instrument is used to perform UV-Vis spectroscopy. It calculates the intensity of light that passes through a sample (I) and compares it to light intensity before passing through the sample (I_o). The transmittance is defined as the ratio I/I_o, usually expressed as a percentage (%).

There are two types of spectrophotometers like single-beam or double-beam spectrophotometers. All the light travels through the sample in a single beam spectrophotometer, and by removing the sample, I_o can be determined. However, in a double-beam instrument, the light is split into two beams. One beam travels through the sample, and the other beam is used as a reference. The sample and reference beams are measured simultaneously in specific double-beam instruments with two detectors (photodiodes).

A plot of light absorbance or transmittance versus wavelength in various ultraviolet or visible regions is known as an ultraviolet-visible spectrum. The wavelengths of absorption peaks help to identify the functional groups within a molecule because they can be compared with the types of bonds in a given molecule. In the present thesis, JASCO V-730 Spectrophotometer located at the Department of Chemistry, Faculty of Science, Maharaja Sayajirao University of Baroda, Vadodara, has been used in transmittance mode with a wavelength range of 200 to 800 nm, with a slit width of 2.0 nm, to perform UV-Visible spectroscopy on grown crystals.

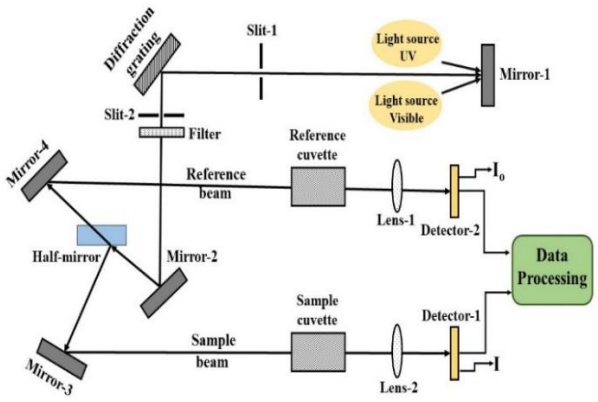

Figure 3(a). Schematic diagram of UV-Visible spectroscopy

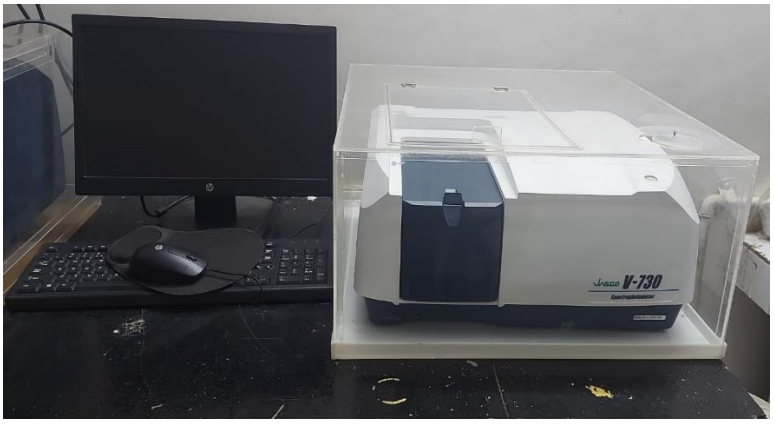

Figure 4(b). JASCO V-730 Spectrophotometer

8. Photoluminescence (PL) Spectroscopy:

Luminescence is a process in which certain substances emit light after absorbing different energies without generating heat. However, the wavelength of the emitted light is determined by the luminescent material, not by incident radiation [13]. Luminophors or phosphors are substances that produce luminescence. The luminescence of phosphors can be described using an energy band model that includes valence and conduction bands and localized energy levels in forbidden regions between the bands. Impurities or imperfections cause localized centres in the material in the host lattice, and these impurities that induce the localized energy levels are called 'Activators'. The radiative transition between the bands is allowed for such activators. In general, such localized energy levels are near the valence band, and electrons occupy these levels, serving as traps for valence band holes. Other impurities can provide levels near conduction bands, and if they're empty, they may serve as electron traps.

In luminescence, a typical excitation mechanism involves raising an electron from the filled band or a filled activator level to the conduction band or from an activator ground level to some higher activator levels. Electrons that enter the conduction bands have two options: they may be trapped or simply return to the activator level. It may return to the conduction band if trapped by absorbing sufficiently thermal or other forms of energy. An electron returning from the conduction band to an empty activator stage gives rise to 'Luminescence'. Energy is passed to the lattice in the form of phonons by a radiation-less transition that occurs to the trapped or free holes. The 'luminescence centre' consists of an activator impurity and a disturbed host lattice, where these transitions occur [14].

8.1 Photoluminescence's fundamental mechanism:

The effect of luminescence in solids occurs when the electronic states of solids are excited by an external energy source, and the excited energy is emitted as light. Photoluminescence is a phenomenon that occurs when energy is obtained from short-wavelength light, typically ultraviolet light. Depending on the electronic band transitions, photoluminescence involves two processes: fluorescence and phosphorescence. The Jablonski energy diagram and the single exited state diagram of photoluminescence are shown in figures 5(a) and 5(b). There are two monochromators in this system, i.e., the Excitation monochromator and the Emission monochromator. They use both reflective optics to achieve high resolution throughout the entire spectral range while minimizing spherical aberrations and re-diffraction. Each monochromator's entrance and exit ports have continuously adjustable slits. The bandpass of light incident on the sample is determined by the width of the slits on the excitation monochromator. The signal detector uses the emission monochromator slits to control the intensity of the fluorescence signal recorder.

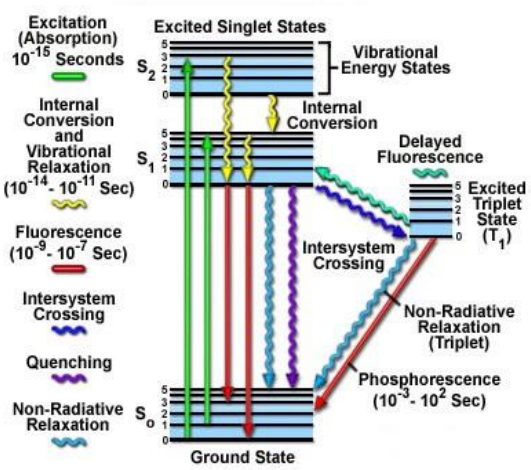

Figure 5 (a). The Jablonski energy diagram

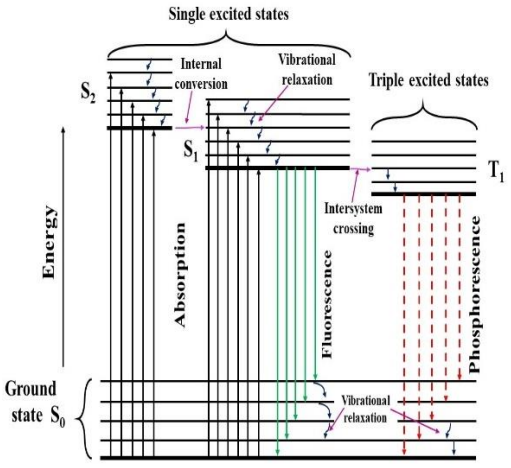

Figure 5 (b). Single excited states in Photoluminescence

There are two distinct forms of photoluminescence: **1)** Intrinsic and **2)** Extrinsic luminescence. In intrinsic photoluminescence, luminescence originates from within a pure material or crystal. Extrinsic luminescence occurs when impurities or defects are deliberately incorporated into a phosphor. In the case of ionic crystals, they can be unlocalized or localized. When free electrons in the conduction band and free holes in the valence band of the host lattice participate in the luminescence, it is said to be unlocalized. When a localized luminescent centre restricts the excitation and emission process of the luminescence, a localized type occurs.

A typical fluorescence spectrometer includes wavelength selectors, sample illumination, detectors, and corrected spectra in its laser sources. It can also scan the excitation and emission wavelengths in addition to fluorescence recording. A 150 W ozone-free xenon arc lamp is used as a continuous light source. A diamond-turned oval mirror first gathers the light from the lamp, and then it is focused on the entrance of the excitation monochromator. A quartz window separates the lamp housing from the excitation monochromator. This allows heat to leave the instrument and protects against improbable occurrence of lamp failure.

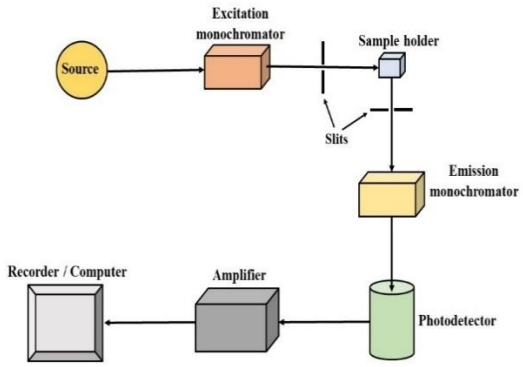

Figure 5(c). Schematic diagram of a fluorescence spectrometer

When considering a slit width, the trade-off is between signal intensity and spectral resolution. If the slits get broader, more light will fall on the sample and detector, and as a result, the resolution will decrease. So, the smaller the slits, the higher the resolution; however, at the expense of signal. After the excitation monochromator exit slit, there is an excitation shutter located. The shutter prevents the sample from photobleaching or photo deterioration caused by prolonged light exposure.

Before the emission monochromator entrance, an emission shutter is mounted to protect the detector from bright light. There are various optional accessories accommodated in the sample compartment. There are fibre optic packages to carry the excitation beam to a remote sample and return the emission beam to the emission monochromator. It has two detectors: a signal detector and a reference detector. A signal detector is used as a photon-counting detector. It is an R928P photomultiplier tube, and it detects the signal and sends it to a photon counting module. The reference

detector monitors the xenon lamp, which compensates for the lamp's wavelength and time-dependent output. This detector, which is located just before the sample compartment, is a UV enhanced silicon photodiode.

A photograph of the Spectrofluoro photometer instrument is shown in figure 5(d). At room temperature, a photoluminescence emission and excitation study of the grown crystals was carried out by the present author using Shimadzu RF-5301 PC Spectrofluorophotometer located at the Department of Applied Physics, Faculty of Technology and Engineering, Maharaja Sayajirao University of Baroda, Vadodara.

Figure 5(d). Shimadzu RF-5301 PC Spectrofluorophotometer

9. Thermogravimetric Analysis (TGA):

A group of thermal analyses calculates a material's physical property as a function of temperature while the substance is exposed to a controlled temperature program. Thermogravimetric analysis (TGA) and differential thermal analysis (DTA) are some examples of thermal analysis. Thermogravimetric analysis (TGA) is a technique in which a change in the weight of a material is measured as a function of temperature or time because it is heated at a controlled rate in a suitable atmosphere.

When a sample is heated to analyze, it undergoes chemical changes such as thermal decomposition, oxidation, and physical changes such as solvent evaporation, sublimation, and other physical processes, many of which decrease the sample's initial weight.

The thermogravimetric curve or TG curve is a plot of mass versus temperature, and the first derivative of it is called a derivative thermo-gram (DTG). The program's inflection point correlates to the derivative thermogram's peak point. The useful details about the sample, like thermal stability and composition, can be derived from the TGA curve.

TG instrument consists of the following main parts: **1)** A sensitive analytical balance, **2)** A temperature programmable furnace, **3)** A purge gas unit is used to create a suitable gas atmosphere, **4)** A microprocessor that controls the instrument, collects data, and displays it.

Since the TGA includes weight shift as a function of temperature, the data collected as a plot of mass or loss of mass in percentage as a function of temperature is referred to as a thermogram, thermal spectrum, or thermal decomposition curve. These thermograms describe a system's thermodynamic properties and physical-chemical kinetics as a function of temperature. Thermogravimetric is commonly used to assess thermal stability, decomposition temperature, oxidative stability, and temperature of desorption and drying, etc.

9.1 Differential thermal analysis (DTA):

The temperature difference between a substance and an inert reference medium is measured as a function of time or temperature in differential thermal analysis. Any transformation that the sample goes through can cause the sample to release or absorb energy, resulting in a temperature deviation from the reference. This energy difference is expressed as a change in enthalpy, either endothermic or exothermic. During a heat-up or cool-down cycle, DTA provides information on the chemical reactions, phase transitions, and structural changes that occur in a sample.

The differential thermocouple output in microvolts on the Y-axis versus the sample temperature in °C on the X-axis is DTA's plot, resulting in DTA. Modern thermo-balances are often well-designed so that it simultaneously records both the DTA signal and the actual thermo-gravimetric measurement.

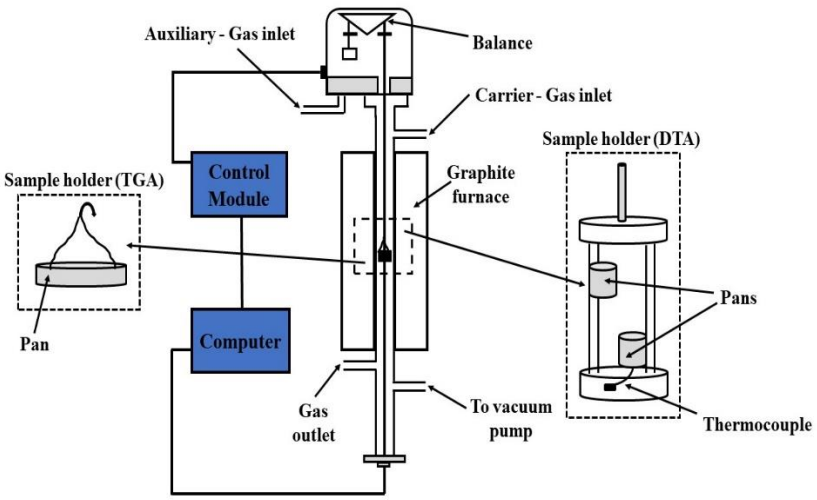

Figure 6(a). Schematic diagram of TGA

After turning on the computer and the thermobalance, the furnace must be opened using the LIFT switch. The measuring head is equipped with two identical pans, one for the reference material and the other for sample substance, each supported by a thermocouple. Two types of pans are used in TGA: **1)** Aluminium pan (Al) and **2)** Platinum pan (Pt). Pt pan is used for a

higher temperature range. If the pan is used earlier, then remove the used pan with care and thoroughly clean it. Place a fine powder of the grown crystals or seed crystal in the sample pan on the right side, and the reference pan is kept empty. The two thermocouples are wired such as to measure the temperature difference between the sample and the air. The reference thermocouple is used to determine the absolute temperature. For best results, good thermal communication between the sample and the heat flux sensor is much needed. Thermo-analytical investigations significantly impact some parameters such as calibration, sample preparation, sample weight, reference material, sample chamber temperature, temperature program, and atmosphere. These parameters should be carefully considered. The TGA experiment was carried out in an air atmosphere at temperatures ranging from room temperature to 500 °C, with a heating rate of 10 °C/min. TA-Evaluation program is used to analyze the collected raw data. TGA study was carried out using TG-DTA SII IN CARP EXSTAR 6000 at the Department of Chemistry, Faculty of Science, Maharaja Sayajirao University of Baroda, Vadodara.

Figure 6(b). TG-DTA SII IN CARP EXSTAR 6000

10. Dielectric Analysis:

Depending on the type of material, every material has its own set of electrical properties, such as dielectric properties, permittivity, permeability, resistivity, conductivity, etc. Dielectric materials are electrical insulators or materials in which an electric field can be sustained with negligible power dissipation. In other words, if a material can store energy when an external electric field is applied, it is classified as “dielectric”. Generally, dielectric materials are insulating materials, and there are no free charges in dielectrics because all electrons are bound to their parent molecules. Due to this, electrons are not released even with standard voltage or thermal energy. Dielectric characteristics play a vital role in understanding crystal

lattice dynamics. Permittivity and permeability are not constant and can vary based on the frequency, molecular structure, temperature, orientation, mixture, and pressure.

10.1 Dielectric Constant (ε_r):

The dielectric constant is the ratio of the capacitance of a capacitor (C) filled with given material to the capacitance of an identical capacitor (C_o) in a vacuum without the dielectric material. It is also defined as the ratio of the dielectric material's permittivity (ε) to the permittivity of vacuum (ε_o). Therefore, it is also known as the relative permittivity (ε_r) of a material.

$$\text{Dielectric constant, K} = \varepsilon_r = \frac{C}{C_o} = \frac{\varepsilon}{\varepsilon_o} \quad (1)$$

The dielectric constant is dimensionless and always greater than 1 as it is just a ratio of two similar quantities. It measures the polarisation in the dielectric material. The dielectric constant is calculated in the present study by using the following formula:

$$\text{Dielectric constant, K= } \varepsilon_r = \frac{t}{\omega A \varepsilon_o}\left[\frac{Z''}{Z'^2 + Z''^2}\right] \quad (2)$$

where, t = the thickness of the crystal, ε_o = the vacuum dielectric constant (permittivity of free space, ε_o = 8.854 x 10−12 F/m), A = the area of the electrode, ZZ' is the real part and Z'' is the imaginary part of complex impedance.

10.2 Dielectric Loss (tan δ):

The dielectric loss is an energy loss that causes a temperature rise in a dielectric placed in an alternating electrical field. It's a calculation of how much energy dielectric absorbs. In other words, it is the electrical energy lost as heat during the polarization process in an applied AC electric field. Dielectric loss or the dissipation factor is the ratio of the imaginary part (ε'') of the relative permittivity to the real part (ε') of the relative permittivity given by,

$$\text{Dielectric loss} = \tan\delta = \frac{\varepsilon''}{\varepsilon'} \quad (3)$$

10.3 A. C Conductivity:

The electrical conductivity of solid electrolytes as a function of frequency can be divided into two categories: frequency-independent direct current conductivity (d. c conductivity, $\sigma_{d.c}$) and frequency-dependent conductivity (a. c conductivity, $\sigma_{a.c}$). Figure 7(a) depicts a standard frequency dependency of conductivity spectrum and shows three distinct regions: **(a)** low-frequency dispersion, **(b)** an intermediate frequency plateau, and **(c)** an extended dispersion at high frequency. The polarization effects at the electrode and crystal

interface are responsible for the difference in conductivity in the low-frequency field. More charge accumulation occurs at the electrode and crystal interface in the low-frequency region, resulting in decreased conductivity. Conductivity is almost frequency independent in the intermediate frequency plateau region and equals d. c conductivity ($\sigma_{d.c}$). The conductivity increases with the frequency in the high-frequency region.

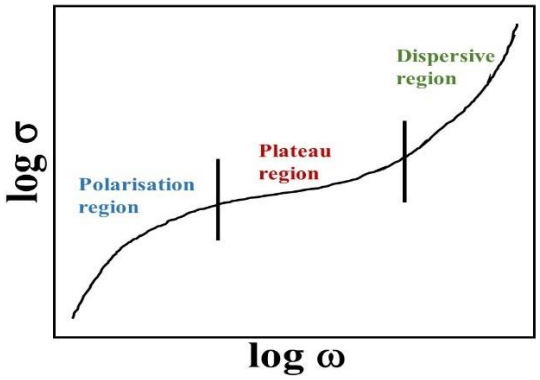

Figure 7(a). Schematic representation of log σ versus log ω

Jonscher's power law relates the frequency-dependent conductivity, or so-called uniform dynamic reaction, to ionic conductivity, as follows:

$$\sigma_{\omega} = \sigma_{o} + A\omega^{s} \quad (4)$$

where, σ_{ω} = a. c conductivity, σ_{o} = limiting zero frequency conductivity or $\sigma_{d.c}$, A = pre-exponential constant = strength of polarizability, ω = 2πf = angular frequency, s = degree of correlation of mobile ions with lattice.

When conductivity is calculated using an a. c frequency technique, the response that characterizes a wide range of materials with different chemical compositions, either crystalline or amorphous, can be written as follows by slightly altering the above equation.

$$\sigma_{(\omega,T)} = \sigma_{d.c}\,(T) + A(T)\,\omega^{s} \quad (5)$$

where, $\sigma_{d.c}$ (T) is the "direct current" (or static, ω = 0) conductivity, A (T) is a factor that depends on temperature but not on ω, and s is an exponent in the range $0 \leq s \leq 1$.

The exponent 's' has been observed to have many forms, including constant, decreasing with temperature, increasing with temperature, and so on, but constantly varying within $0<s<1$. Factor A is referred to as straight of polarizability, and in a many-body interactive system, the exponent s denotes the degree of correlation of mobile ions with the lattice Based on the variation of the s-parameter with the temperature range studied [15,16], various conduction mechanisms are proposed as follows:

1) **Quantum Mechanical Tunneling (QMT):** "s-parameter" is independent of temperature
2) **Non-overlapping Small-Polaron Tunneling (NSPT):** "s-parameter" increases as temperature increases
3) **Correlation Barrier Hopping (CBH):** "s-parameter" decreases as temperature increases
4) **Hopping Over the Barrier (HOB):** "s-parameter" remain unity

10.4 POLARON:

Electrons and holes in a typical covalently bonded crystal can be described as an excellent approximation by assuming that electrons and holes pass through a crystal whose atoms are fixed in place. Of course, electrons and holes will scatter off phonons, but when there are no phonons present (for example, at extremely low temperatures), all ionic displacement is neglected when explaining electron and hole transport and properties. This approach becomes insufficient because the Coulomb interaction between a conduction electron and the lattice ions in ionic crystals results in a heavy electron-phonon coupling. The electron is still surrounded by a cloud of simulated phonons in this case, even though no actual phonons are present. The electron pulls nearby positive ions towards it and pushes nearby negative ions away, resulting in a cloud of virtual phonons.

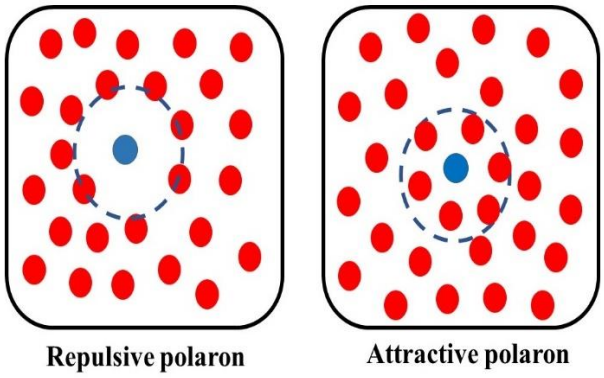

Figure 7(b). Schematic presentation of Polaron

The electron and its virtual phonons can be combined to form a new composite particle known as a "polaron" [17]. In the present research, the author has observed a Correlation Barrier Hopping (CBH) kind of conduction mechanism prevailing for the grown crystals.

The dielectric analysis was carried out using SOLARTRON HIOKI 3532 LCR meter [figure 7(c)] in the frequency range of 10 Hz to 10 MHz in temperature of 323 – 373 K on

crystals. The obtained data were analyzed using Z-view software at the Department of Physics, Faculty of Science, Maharaja Sayajirao University of Baroda, Vadodara.

Figure 7(c). SOLARTRON HIOKI 3532 LCR meter with temperature controller

11. Second Harmonic Generation (SHG) Efficiency:

There has been a substantial quest for possible inorganic, organic, and semi-organic non-linear optical materials as non-linear optics play a vital role in optoelectronics and photonics. The powder SHG test can be used to determine whether the advanced materials are non-linear or not. In 1968, Kurtz and Perry [18] introduced a powder SHG method for a systematic study of second-order nonlinearity. This is a pivotal factor for characterizing materials before embarking on the lengthy process of developing huge optically high-quality crystals. The schematic diagram in figure 8 shows the working of Kurtz and Perry powder SHG measurement. The powdered sample is targeted by a Q-switched Nd: YAG laser beam with a wavelength of 1064 nm and a pulse width of 10 ns. This laser has two modes of operation: **1)** The laser emits a single 8 ns pulse in single-shot mode, and **2)** The laser emits a continuous train of 8 ns pulses at a repetition rate of 10 Hz in the multi-shot mode. The powdered samples are airtight packed in micro-capillary tubes with uniform bores of around 1.5 mm diameter. In this experiment, a mirror and beam splitter was used to generate a beam with pulse energies of around 1.2 mJ. After passing through an IR reflector, the input laser beam was focused on the powdered microcrystalline sample packed in a capillary tube. The light emitted by the sample was determined by the assembly of a photodiode detector and oscilloscope. For comparison, microcrystalline urea or KDP powder is placed in a related capillary tube with one end sealed. The sample's second harmonic output is compared to the intensity of KDP or urea.

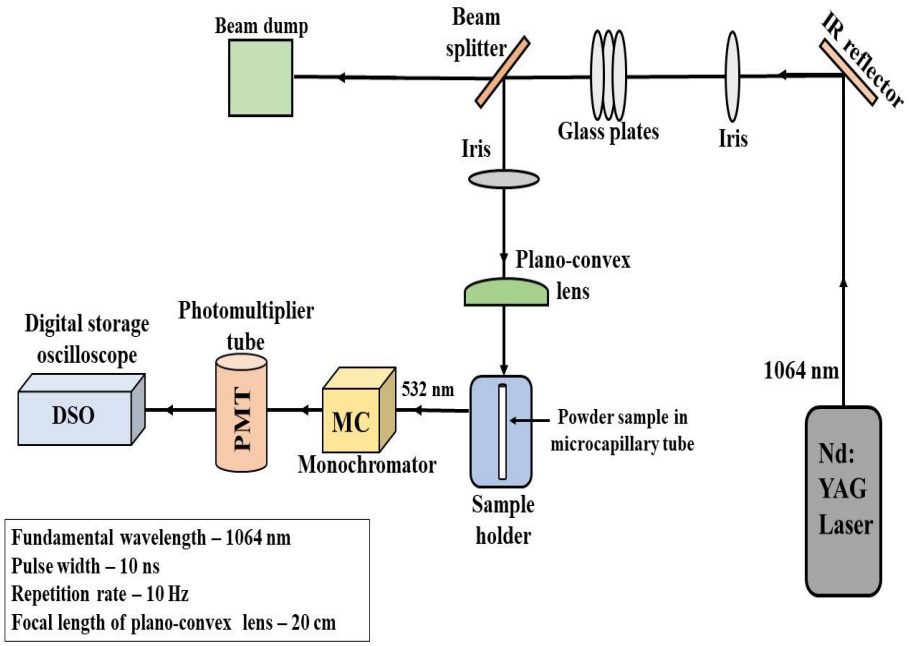

Figure 8. Schematic diagram of SHG experiment

The present author has used ratio of Output energy of sample to the output energy of KDP to measure the relative SHG efficiency of pure and amino acid doped KDP crystals.

The present author calculated the relative SHG efficiency of grown crystals using a Q-Switched High Energy Nd: YAG Laser with input energy 1.2 mJ at the Department of Inorganic and Physical Chemistry, Indian Institute of Science, Bangalore.

References:

1. H. A. Buckley, *"Crystal growth"*, John Wiley and Sons, New York (1952).
2. J. C. Brice, *"The growth of crystals from liquids"*, North-Holland Publishing Co., Amsterdam (1973).
3. W. K. Burton, N. Cabera and F. C. Frank, *Philosophical Transactions of the Royal Society of London. Series A, Mathematical and Physical Sciences*, **243** (1951) pp. 299-358.
4. K. A. Jackson, *"Liquid metals and solidification"*, American Society of Metals, Cleveland, (1958) pp. 174-186.
5. J. D. H. Donnay and D. Harker, *American Mineralogist*, **22** (1937) pp. 446-467.
6. F. C. Philips, *"An Introduction to Crystallography (3rd Edition)"*, London: Longmans Green (1946).
7. P. Wartman and W. G. Perdok, *Acta Crystallogr.*, **8** (1955) pp. 49-52.
8. H. Lipson, Steeple, *"Interpretation of X-ray powder diffraction pattern"*, London (Macmillan) and New York (St. Martins Press) (1970).
9. L. V. Azaroff, M. J. Buerger, "*The Power Method in X-ray Crystallography*", McGraw-Hill, New York, USA (1958).
10. N. Colthup, L. Daly, S. Wiberley, *"Introduction to Infrared and Raman Spectroscopy (3rd Edition)"*, Academic Press, New York (1990).
11. G. D. Pitt, D. N. Batchelder, R. Bennett, R. W. Bermett, I. P. Hayward, B. I. E. Smith, K. P. J. Williams, Y. Y. Yang, K. I. Baldwin, S. Webster, *IEE Proc. – Sci. Meas. Technol.*, **152**(6) (2005) pp. 241-318.
12. M. Schmitt, J. Popp, J. Raman Spectrosc., **37** (2006) pp. 20-28.
13. D. R. Vij (Ed.), *"Luminescence of solids",* Plenum Press, New York (1998).
14. S. W. S. McKeever, *"Thermoluminescence of Solids"*, Cambridge University Press, Cambridge, USA (1985).
15. A. Kahouli, A. Sylvestre, F. Jomni, B. Yangui, J. Legrand, *J. Phys. Chem. A,* **116**(3) (2012) pp.1051-1058.
16. S. Murugavel, M. Upadhyay, *J. Ind. Inst. Sci.*, **91**(2) (2011) pp. 303-318.
17. J. T. Devreese, *"Polarons",* Digital Encyclopedia of Applied Physics, Wiley, (2008).
18. S. K. Kurtz, T. T. Perry, *J. Appl. Phys.*, **39** (1968) pp. 3798-3813.